LIMNOLOGY and OCEANOGRAPHY

ASLO

Limnol. Oceanogr. 9999, 2025, 1–14

doi: 10.1002/lno.70005

RESEARCH ARTICLE

Differences in bed elevation shape subtidal mussel bed stability under high-energy hydrodynamic events

Zhiyuan Zhao,[1*] **Jaco C. de Smit**,[2] **Jacob J. Capelle**,[3] **Tim Grandjean**,[1] **Mingxuan Wu**,[1] **Theo Gerkema**,[1] **Johan van de Koppel**,[1] **Tjeerd J. Bouma**[1,2,4]

[1]Department of Estuarine and Delta Systems, Royal Netherlands Institute for Sea Research, Yerseke, The Netherlands; [2]HZ University of Applied Sciences, Building with Nature Group, Vlissingen, The Netherlands; [3]Wageningen Marine Research, Yerseke, The Netherlands; [4]Faculty of Geosciences, Department of Physical Geography, Utrecht University, Utrecht, The Netherlands

Abstract

Escalating high-energy hydrodynamic events, like storms, represent a significant manifestation of global climate change, causing detrimental impacts on various ecosystems and potentially triggering thresholds that result in abrupt shifts in ecosystem states. Despite the potential of such thresholds, few studies have explicitly addressed them. This gap is particularly notable for subtidal ecosystems due to technological challenges in detecting responses of organisms enduring constant submersion. This study focused on subtidal soft-bottom mussel beds through the development of Biophys loggers for in situ monitoring of the fine-scale behavior of mussel clusters under hydrodynamic disturbances and a statistical model based on an 11-yr dataset to perform regional-scale assessments of mussel bed stability. Multisite monitoring in the Dutch Wadden Sea revealed spatial heterogeneity in mussel bed mobility threshold (i.e., near-bed orbital velocity inducing mussel movement), with predictable patterns along elevation gradients. Stability assessment in this region demonstrated that mussel beds in shallower areas (i.e., at higher bed elevations) exhibited higher stability than those in deeper areas, a difference that was attributed to the longer return interval of the mobility thresholds in shallow regions. These findings suggest that conditions such as bed elevation can modulate the stress tolerance of mussels and thereby influence the stability of subtidal soft-bottom mussel beds. This study provides an approach for assessing mussel bed stability, which can also be extended to other comparable ecosystems, such as oyster reefs, to address their stability under climate change, thereby informing strategic management.

Disturbance regimes within ecosystems are changing due to anthropogenic climate change (Hawkins et al. 2023). Specifically, discrete high-energy hydrodynamic events such as storms are increasing in frequency and intensity in some regions (Kossin et al. 2020; Wang and Toumi 2022). Although ecosystems are resilient to some levels of stress, catastrophic shifts in structure and functionality may arise after a critical stress threshold, making them less likely to revert to their former states (Scheffer et al. 2012; Rietkerk et al. 2021). Among the most affected ecosystems involve organisms that are ecosystem engineers, such as species that form shellfish reefs, seagrass beds, and salt marshes (Donker 2015; Commito et al. 2018; Zhao et al. 2022). These ecosystem engineers play a vital role by providing habitats, immobilizing carbon, and safeguarding coastlines, that is, their structure and function (Temmink et al. 2022; Crotty et al. 2023). With the anticipated increase in high-energy hydrodynamic events, it is imperative to determine their effects on ecosystem engineers, thereby informing strategic management aimed at mitigating the ongoing trends of population collapse and the loss of essential ecosystem services (Neilson et al. 2020; Schotanus et al. 2020).

*Correspondence: zhiyuan.zhao@nioz.nl

Associate editor: Josef Ackerman

Data Available Statement: The data that support the findings of this study are openly available in 4TU. Research Data Repository at https://doi.org/10.4121/5e0d79c5-cf72-4868-a3dc-a4aa9d9a59ce.

Mussel beds are structures produced by coastal ecosystem engineers and are subjected to hydrodynamic disturbances in soft sediments or hard substrates (such as rocks) in the intertidal and subtidal zones (Ricklefs et al. 2020; Crotty et al. 2023). Particularly for subtidal soft-bottom mussel beds, mussels often employ byssal threads to attach to conspecifics, forming extensive and closely-knit aggregations that contribute to long-term persistence (Commito et al. 2014; de Paoli et al. 2017). Population losses in these mussel beds, characterized by the dislodgement of individuals or clusters from the aggregations, have been linked to hydrodynamic disturbances (de Paoli et al. 2015; Capelle et al. 2019) generated by current- and wave-generated shear forces exceeding the attachment strength of mussels (Carrington et al. 2009; Donker 2015). Given the impacts of population loss on local biodiversity and the mussel bottom mariculture sector, mitigating the effects of high-energy hydrodynamic events has been the focus of soft-bottom mussel bed conservation for decades (Wilcox et al. 2018; Schotanus et al. 2020). Nonetheless, predicting the location, timing, and extent of the population losses remains challenging, particularly for mussel beds in subtidal areas (Carrington et al. 2009; Avdelas et al. 2021). Addressing these challenges requires in situ observations of the stability of subtidal soft-bottom mussel beds under various hydrodynamic gradients across diverse temporal and spatial contexts.

The stability of soft-bottom mussel beds depends on the balance between hydrodynamic intensity and the mussel's ability to withstand it (Carrington et al. 2009; Donker 2015). It can be quantified as the critical hydrodynamic force beyond which mussel movement increases abruptly, known as the mobility threshold (Fig. 1). Mussel beds characterized by a higher mobility threshold have the capacity to endure hydrodynamic disturbances, thus maintaining relatively stable populations (Fig. 1). Conversely, mussel beds with a lower mobility threshold often experience the dislodgement of mussel clusters during hydrodynamic disturbances, leading to increased landscape fragmentation (Fig. 1), which in turn exacerbates the erosion of mussel bed stability (Bertolini et al. 2019). The ongoing dislodgement of mussel clusters could, in principle, lead to the partial or complete collapse of the mussel beds (Fig. 1). Variations in mobility thresholds among beds may arise from mussel acclimation to the contrasting physical conditions among habitats (Schotanus et al. 2019; Manríquez et al. 2021), such as bed elevation, near-bed hydrodynamics, and water quality, as reflected in changes in byssal strength and aggregation patterns (Moeser et al. 2006; Commito et al. 2014). This acclimation might also fluctuate depending on biotic characteristics such as mussel size and density (Schotanus et al. 2019) as well as predator pressure (Manríquez et al. 2021), which vary between microsites, causing differences in mobility thresholds within a confined spatial domain. Some studies have utilized methods such as trawl sampling, sonar scanning, and remote-operated vehicle imaging to monitor population dynamics within subtidal mussel beds (Capelle et al. 2017; Ricklefs et al. 2020; Bridger et al. 2022), whereas the ongoing movement of mussel clusters over time at small scales has been largely ignored. Nevertheless, the coupling of the latter with the time-series evolution of hydrodynamic forces is indispensable for accurately quantifying mussel bed stability (Carrington et al. 2009; Donker 2015).

In this study, we aimed to determine the stability of subtidal soft-bottom mussel beds under hydrodynamic disturbances through in situ monitoring and to apply these insights to perform risk assessments in a typical region. Specifically, we hypothesized that the stability of these mussel beds is closely linked to changes in the motion of mussel clusters, which are expected to (1) occur when specific hydrodynamic thresholds are exceeded and (2) exhibit noticeable spatial heterogeneity. To test this hypothesis, we developed retrievable Biophys loggers for the long-term, high-frequency monitoring of mussel cluster behavior under hydrodynamic disturbances. The Dutch Wadden Sea, inhabited by subtidal soft-bottom mussel beds, was employed as a model system, with eight sites selected for the deployment of Biophys loggers. The data were expected to facilitate the quantification of the mobility threshold for each mussel bed and establish a relationship between inter-site variations in the mobility threshold and key environmental features. Furthermore, a statistical model was constructed to reproduce wave regimes over the past 11 yr (2011–2021) and calculate the return interval (i.e., average occurrence frequency) of the site-specific mobility threshold. Shorter return intervals of mobility thresholds at specific locations indicate lower stability in mussel beds and thus a higher risk of fragmentation or collapse during high-energy hydrodynamic events.

Materials and methods

Biophys loggers: Composition and calibration

Retrievable Biophys loggers were used in this study for the in situ monitoring of mussel bed mobility at high frequencies. The Biophys loggers incorporated seven compact accelerometers (MSR-145B4) and one pressure sensor (OSSI-010-003C), allowing the separate recordings of movement acceleration and wave regimes over time in a mussel bed. The accelerometers are comparable in size ($5.3 \times 1.6 \times 1.1$ cm) and weight (18 g) to that of individual mussels. Ten live juvenile mussels (with an average shell length of 4.8 ± 0.1 cm) were glued to each accelerometer using waterproof adhesive (i.e., 2k polyurethaanlijm, Bison) to create mussel clusters of natural size (Fig. 3a), enabling the accelerometers to move along with the mussel clusters as they were incorporated into an existing mussel bed. Once the mussel clusters moved, the contained accelerometer recorded the timing of the occurrence and acceleration in multiple directions. Coupled with the wave dynamics captured simultaneously by the pressure sensor, we identified the critical hydrodynamic threshold responsible for mussel cluster movement.

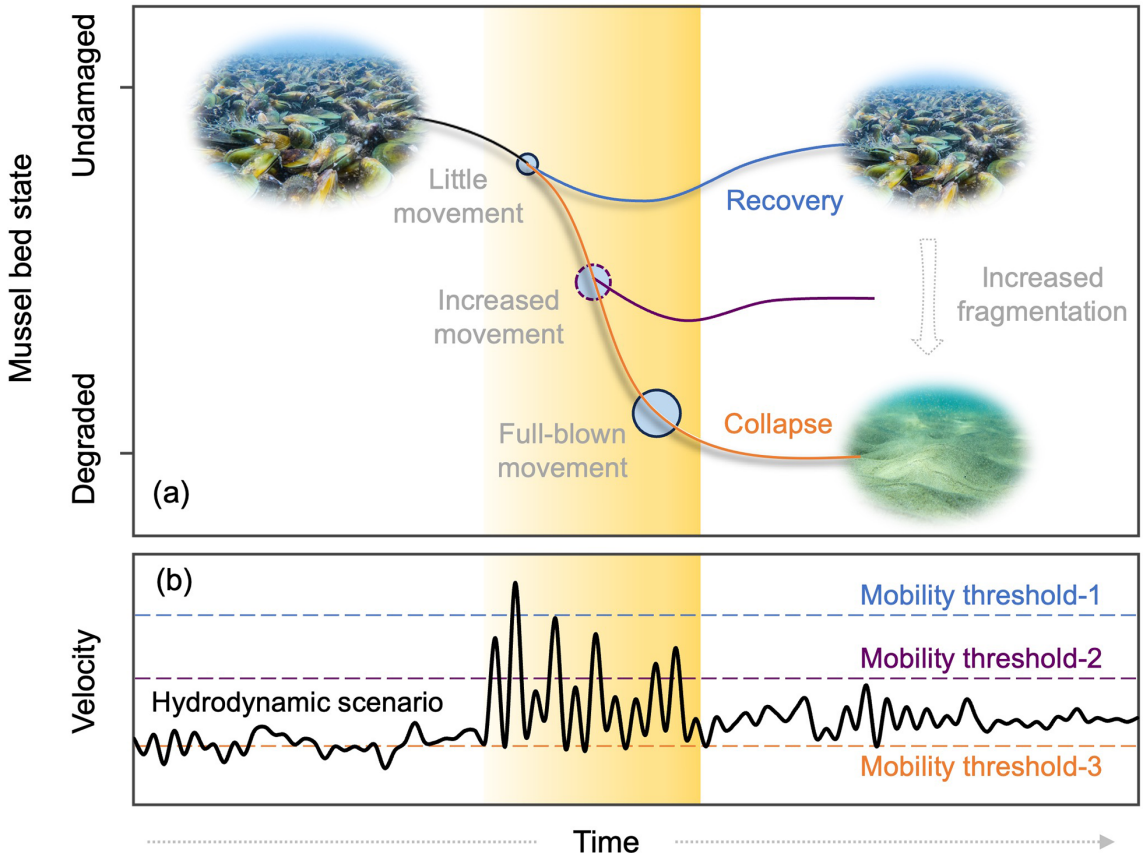

Fig. 1. Schematic diagram illustrates the diverse fates of soft-bottom mussel beds in the subtidal zone (**a**). Under an identical hydrodynamic scenario (black line in **b**): (1) Mussel beds with the mobility threshold-1 are highly stable, with few mussels undergoing movement and the ability to recover when the velocity falls below the threshold (blue line in **a**, **b**). (2) Mussel beds with the mobility threshold-3 are highly unstable, with most mussels in motion and the potential to collapse as long as the velocity remains above the threshold (orange line in **a**, **b**). (3) Mussel beds with the mobility threshold-2 become fragmented due to mussel movement (purple line in **a**, **b**). They may recover during subsequent calm hydrodynamic periods or collapse during subsequent strong hydrodynamic periods. The outcome depends on the value of the mobility threshold-2; the lower it is, the more mussels are in motion, leading to greater fragmentation of the mussel bed and, consequently, a higher likelihood of collapse under high-energy hydrodynamic events.

Calibration was conducted using a flume facility at the Royal Netherlands Institute for Sea Research before the field campaign to discern the motion state of mussel clusters from accelerometer readings. The flume comprises an oval racetrack measuring 17.5 m in length and 0.6 m in width (for more details, *see* Zhao et al. 2022), designed to reproduce typical hydrodynamic conditions found in the field under controlled settings. In the straight test section of the flume, an evenly distributed mussel bed (1.6 × 0.6 m) with a spatial density of 10 kg m^{-2} was established on mixed substrates composed of sand and cockle shells, with a water depth of 0.32 m (Supporting Information Fig. S1). Mussel bed density and substrate type involved were within the range of the Dutch Wadden Sea (Capelle et al. 2019). Five mussel clusters containing accelerometers were placed onto the mussel bed and allowed to aggregate under gentle waves (near-bed orbital velocity = 0.24 ± 0.01 m s^{-1}) for 3 d. During this period, the surrounding mussels attached to the mussel clusters formed a homogeneous pattern within the mussel bed, as expected for this density (Bertolini et al. 2019). Following the aggregation phase, the flume was run at its maximum achievable wave setting (near-bed orbital velocity = 0.47 ± 0.02 m s^{-1}) for 1 d to initiate the movement of mussel clusters and establish a stable motion state. The flow velocity and wave height during the flume run were measured using acoustic Doppler velocimeters (Nortek AS) and pressure sensors (Druck PTX 1830), respectively.

Field campaign: Measuring mussel bed stability under diverse hydrodynamic settings

Study area

The Wadden Sea, which extends approximately 500 km along the coasts of the Netherlands, Germany, and Denmark, is a typical shallow estuarine area bordered by the North Sea and divided by a series of small barrier islands. The bulk of the water flux enters through narrow deep inlets propelled by tides and spreads through an extensive network of branching gullies (Donker 2015). The seabed primarily consists of soft

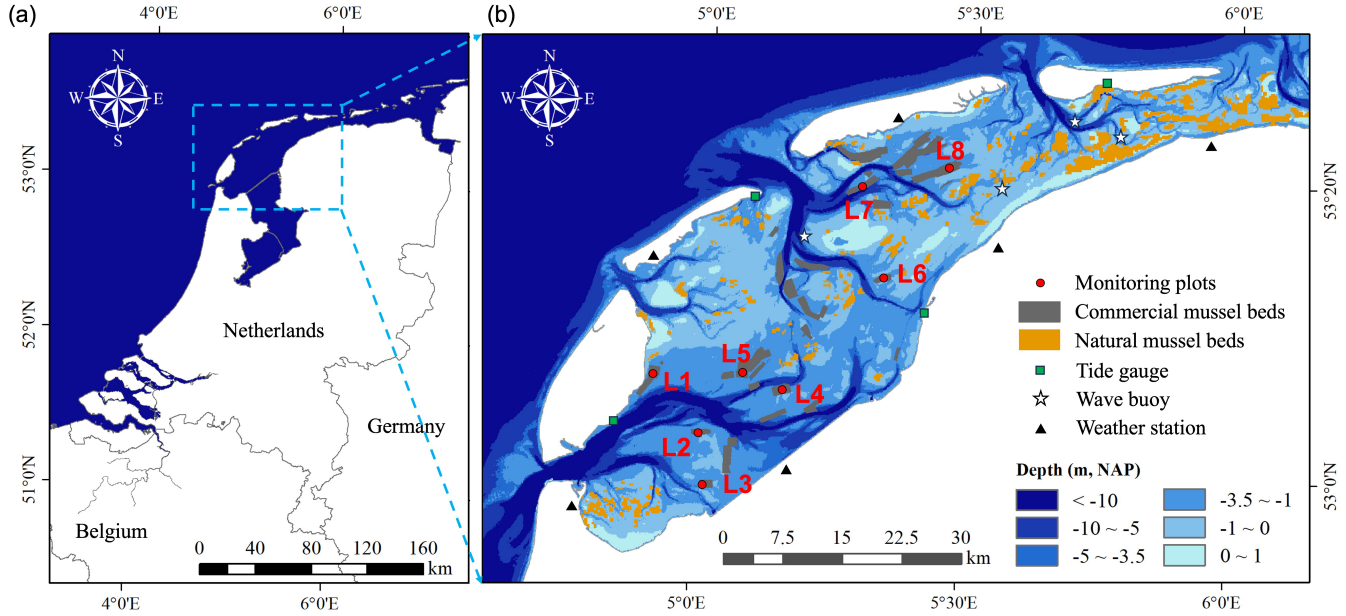

Fig. 2. (**a**) Geographical location of the Dutch Wadden Sea. (**b**) Spatial distribution of monitoring plots with Biophys loggers, as well as mussel beds, tidal gauges, wave buoys, and weather stations, within the Dutch Wadden Sea.

sediments, varying from coarse sands in inlets and tidal gullies to fine mud in shallow regions near the mainland and tidal watersheds (Troost et al. 2022). Our study focused on the subtidal area of the Dutch Wadden Sea (Fig. 2a), where in some years a vast population of natural mussel bed thrives (Smaal et al. 2021). This region also contains the world's largest subtidal mussel bottom-culture plots, encompassing a total area of 3329 ha (Capelle et al. 2017). Eight spatially dispersed

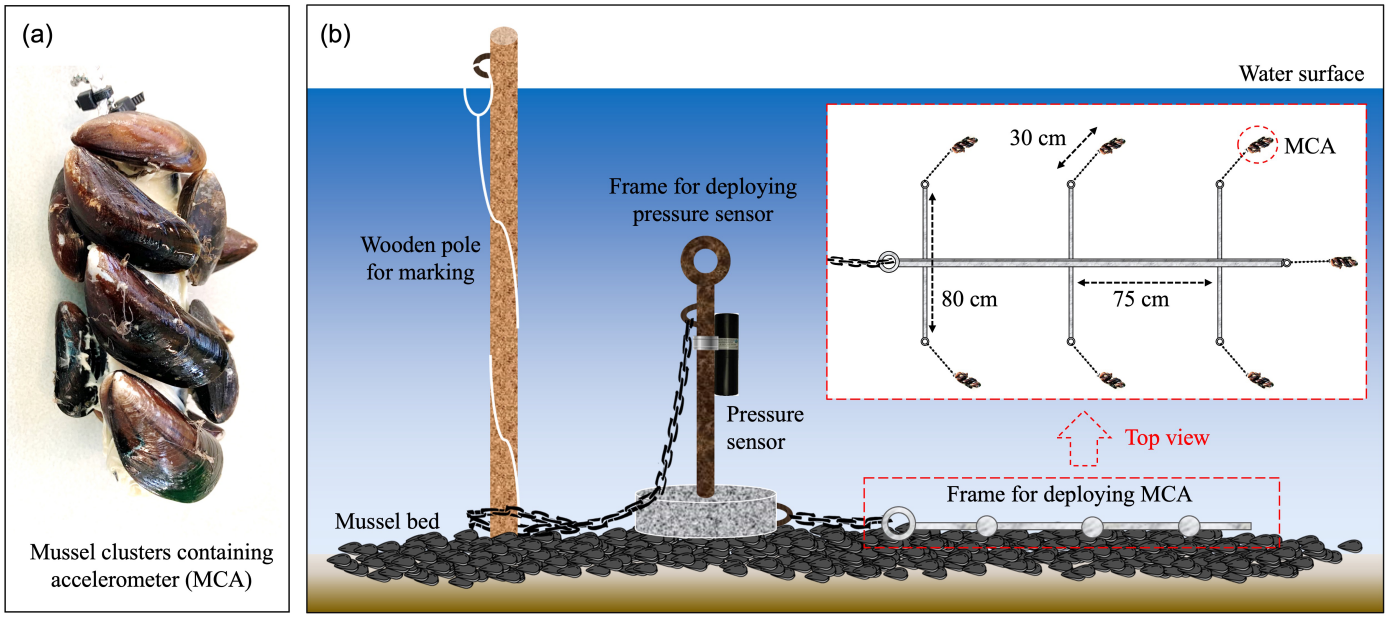

Fig. 3. (**a**) Live juvenile mussels were glued to an accelerometer to form naturally sized clusters, allowing the accelerometer to move with the clusters and record the associated movement intensity as they aggregated on an existing mussel bed. (**b**) The setup for in situ monitoring with Biophys loggers involved using two frames to deploy the components: one pressure sensor and seven mussel clusters containing accelerometers (MCA). These frames were connected by iron chains and secured to a permanently fixed wooden pole. All iron chains were submerged, and a rope wrapped around the wooden pole allowed the chains to be lifted for the retrieval of the frames with Biophys loggers.

commercial mussel beds corresponding to distinct hydrodynamic environments were selected for deployment of the Biophys loggers (Fig. 2b; *see* Fig. 6 for hydrodynamic intensities at each location). All eight beds were established according to industry standards at approximately the same time of year by depositing juvenile mussels collected from suspended collectors (Zhao et al. 2024). All beds had a similar age (< 1 yr) and mass per unit area (ca. 5 kg m^{-2}) and were regularly cleaned of starfish predators as part of the cultivation method. Biophys loggers were deployed in the central area of each mussel bed to minimize edge effects.

Deployment and retrieval of Biophys loggers

A set of Biophys loggers was deployed on each mussel bed between November 26, 2022 and November 28, 2022. During deployment, the seven mussel clusters containing accelerometers were secured to the endpoints of a "fishbone-like" shaped frame using 30-cm ball chains, with the frame endpoints spaced 80 cm apart to prevent interference between clusters (Fig. 3b). The frame was connected to an iron chain, the end of which was looped over a wooden pole and sank to the bottom to prevent it from disturbing the local hydrodynamic environment by swinging into the water column (Fig. 3b). A nylon rope was fastened to the end of the chain and wrapped around the wooden pole up to the water surface to facilitate the lifting of the chain and attached frame during retrieval (Fig. 3b). The pressure sensor was deployed 0.5 m above the bottom using a bottom-weighted frame and connected to the wooden pole using an iron chain in the same manner for easy retrieval.

The accelerometers were configured to record the motion acceleration of mussel clusters at 25-s intervals, whereas the pressure sensors were programmed to measure water pressure at a frequency of 10 Hz during 7.5-min bursts with 15-min intervals between them. To cover the storm season and maximize the capture of high-energy hydrodynamic events, Biophys loggers were left in place for approximately 5 months and retrieved between April 30, 2023 and May 1, 2023. At four of the eight locations, a partial loss of accelerometers occurred because of frame fractures during retrieval. Consequently, each location had at least three accelerometers paired with a pressure sensor to extract site-specific mobility thresholds.

Data analysis

The accelerometers measured gravitational acceleration (m s^{-2}) along the *x*-, *y*-, and *z*-coordinates, based on which the orientation changes (δ_{ori}) of mussel clusters from each measurement can be calculated with the following formula:

$$\delta_{ori} = \sqrt{\triangle_{a,x}^2 + \triangle_{a,y}^2 + \triangle_{a,z}^2} \quad (1)$$

where $\triangle_{a,x}$, $\triangle_{a,y}$, and $\triangle_{a,z}$ are the changes in gravitational acceleration in the *x*-, *y*-, and *z*-directions, respectively, between subsequent measurements (e.g., $\triangle_{a,x} = a,x(t) - a,x(t-1)$, where a,x represent the gravitational acceleration in the *x*-direction). Due to the accelerometer's relative low measurement frequency compared to wave periods, a single δ_{ori} measurement does not effectively represent all actual mussel movements. That is, multiple changes in orientation may have occurred during the time that a wave passes, while δ_{ori} presents the shift from the initial to the final orientation. Therefore, δ_{ori} was summed over a 30-min rolling window to obtain a quantitative proxy for the movement of mussel clusters, called movement intensity (MI; m s^{-2}):

$$MI = \sum_{i=1}^{N} \delta_{ori,i} \quad (2)$$

where $\delta_{ori,i}$ is the orientation changes (δ_{ori}) at the *i*th measurement, and *N* is the number of measurements within the 30-min rolling window.

Pressure measurements were converted into water depths and significant wave heights (Donker et al. 2013). The near-bed orbital velocity (*u*) was calculated from the water depth and significant wave height using linear wave theory to indicate the local hydrodynamic intensity (Soulsby 2006):

$$u = \frac{\omega h_s}{2\sinh[kd]} \quad (3)$$

where ω is the wave orbital speed (rad s^{-1}), h_s is the significant wave height (m), *d* is the water depth (m), and *k* is the wave number, which is calculated as:

$$k = \frac{2\pi}{L} \quad (4)$$

where *L* is the wavelength (m), which is calculated iteratively from the wave dispersion relation:

$$L = \frac{gT^2}{2\pi}\tanh\left[\frac{2\pi d}{L}\right] \quad (5)$$

where *g* is the gravitational acceleration (m s^{-2}) and *T* is the wave period (s).

The movement data of the mussel clusters were resampled at 15-min intervals using a mean-based approach. These data, based on the accelerometer calibration results, were further binarized to represent the mussel states—0 indicates a stable state (i.e., mussels remain at the bottom), whereas 1 signifies a dislodged state (i.e., mussels move with the current). Four-parameter logistic regression (incorporating the lower asymptote, upper asymptote, inflection point, and slope; Eq. 6) was applied to establish the relationship between mussel MI (Eq. 2) and hydrodynamic intensity (*u*; Eq. 3) at each location. This approach allowed for the identification of the site-specific mobility threshold, defined as the hydrodynamic intensity at which mussel cluster states transition sharply, corresponding to the inflection point of the logistic regression curve.

$$\mathrm{MI} = \frac{A1 - A2}{1 + \left(\frac{u}{\mathrm{EC50}}\right)^{p}} + A2 \tag{6}$$

where $A1$, $A2$, and EC50 are the lower asymptote, upper asymptote, and inflection point of the regression curve, respectively; p is the slope factor.

To identify the key factors associated with site-to-site variability in the mobility threshold, the average environmental characteristics for each location, including elevation, hydrodynamics, chlorophyll *a* (Chl *a*) concentration, and salinity, were gathered from open-access sources. Specifically, elevation and hydrodynamic data were obtained from the Ecotope map provided by Rijkswaterstaat (https://maps.rijkswaterstaat.nl) and were expressed in terms of elevation (*m*, Normal Amsterdam Level), maximum current velocity ($\mathrm{m\ s^{-1}}$), and average wave-induced orbital velocity ($\mathrm{m\ s^{-1}}$). The modeled data for seawater salinity were extracted from the Copernicus Marine Ocean Global Reanalysis product (DOI: https://doi.org/10.48670/moi-00021) and computed as annual averages for each location. The Chl *a* content in the water column, derived from time-series remote sensing analysis, was obtained from the Coastal Observing System for Northern and Arctic Seas (https://codm.hzg.de/codm/) data portal and was calculated as annual averages for each location. Pairwise correlation analysis was performed to identify potential correlations among environmental variables. Multivariate linear models were used to examine site-specific mobility thresholds related to local environmental characteristics. All data analyses were performed using either Python (version 3.11.5) or R (version 4.3.2).

Wave statistical model: Assessing the stability of subtidal mussel beds

A one-dimensional wave statistical model was constructed to assess the stability of subtidal mussel beds in the Dutch Wadden Sea. Using this model, the daily maximum near-bed velocity across the region for the past 11 yr (2011–2021) was reproduced and compared with the site-specific mobility thresholds. The latter were extrapolated using the quantified relationship between the elevation and mobility thresholds obtained from in situ monitoring. This extrapolation of the mobility threshold was restricted to the elevation range encompassed by field monitoring, which covered the distribution of subtidal mussel beds in the Dutch Wadden Sea (Fig. 2b). If the daily maximum near-bed velocity surpasses the mobility threshold, it signifies the movement of the mussel clusters. The return interval of hydrodynamic events surpassing the mobility threshold over the 11-yr period was calculated for each site using extrapolated mobility thresholds, providing an estimate of the local instability risk, that is, the potential for mussel clusters to be dislodged from the bed. Essentially, a shorter return interval of the mobility threshold implies a higher risk of mussel-bed instability, whereas a longer return interval suggests a lower instability risk.

The constructed model computed the wave height using 10-min water depth data from four tidal stations and hourly wind data from six meteorological stations (Fig. 2b), sourced from the Rijkswaterstaat and Koninklijk Nederlands Meteorologisch Institute. Specifically, the Youngh–Verhagen equation describes the generation of wind waves over areas with limited depth (Young and Verhagen 1996), as follows:

$$H^{*} = 0.24\left\{\tanh\left[0.49(d^{*})^{0.75}\right]\tanh\left[\frac{0.0031(F^{*})^{0.57}}{\tanh\left[.49(d^{*})^{0.75}\right]}\right]\right\}^{0.87} \tag{7}$$

where H^{*} is the dimensionless wave height, d^{*} is the dimensionless water depth, and F^{*} is the dimensionless wind fetch. F^{*} and d^{*} are the inputs calculated from the fetch and water depths as follows:

$$d^{*} = \frac{gd}{W^{2}}, F^{*} = \frac{gF}{W^{2}} \tag{8}$$

where F is the fetch (m) and W is the wind speed ($\mathrm{m\ s^{-1}}$). The fetch is calculated using a publicly available Python script (https://www.datainwater.com/post/wind_fetch/). The full range of tidal elevations occurring in the Dutch Wadden Sea, using 30 cm depth intervals, was considered, as fetch changes with the emergence and submergence of intertidal areas. Sixteen wind direction intervals were considered, each based on the average fetch of 12° × 2° increments (i.e., 0° for a north wind is the average fetch of 12°, with 2° direction increments ranging from −12° to +12°). This approach was used to eliminate unrealistic "fetch shading" from barrier islands and emergent intertidal areas, and implicitly account for wave diffraction, which is not included in the wave height calculations. The significant wave height, h_s (m), was calculated from H^{*} as follows:

$$h_s = \frac{H^{*}W^{2}}{g} \tag{9}$$

The near-bed orbital velocity was then computed using Eqs. 3–5 based on linear wave theory. The existing data on significant wave height, monitored in situ at 10-min intervals by four spatially dispersed wave buoys belonging to Rijkswaterstaat (Fig. 2b), were used to evaluate the performance of the constructed wave model (*see* Supporting Information Figs. S2, S3 for the evaluation results).

The final model output, namely, the return interval of the mobility threshold representing the risk of mussel bed instability, was evaluated by comparing it with the in situ survey data documented by Capelle et al. (2016). They recorded the

population loss rates in 42 commercial mussel bottom culture plots in the Dutch Wadden Sea between 2009 and 2012 (51 available records). A linear correlation was employed to assess the alignment between the model output and the documented survey results.

Results

Determination criteria for mussel movement

In the flume calibration tests, mussel clusters containing accelerometers remained stable with minimal changes in orientation during the acclimation phase; however, frequent shifts in orientation were observed upon dislodgement after exposure to increased hydrodynamics (Fig. 4a). Following the grouping and averaging of mussel MI in both stable and dislodged phases, an average MI of 10.2 m s^{-2} was recognized as the criterion for classifying mussel states (Fig. 4b). Mussel clusters were considered to be in motion when their movement intensities exceeded this criterion.

Spatial variation of the mobility threshold in subtidal mussel beds

Data from the retrieved Biophys loggers showed that at one of the eight locations (i.e., L7; Fig. 2b), mussel clusters containing accelerometers failed to aggregate into local mussel beds. This failure to aggregate was evident as they always moved regardless of the near-bed orbital velocity (Fig. 5b). In two other locations (L3 and L8; Fig. 2b), mussel clusters containing accelerometers aggregated into local mussel beds but never moved because of weak local hydrodynamic forces (Fig. 5a). Consequently, these three locations were excluded as unsuitable for quantification of the mobility threshold.

In the remaining five locations, the mussel clusters containing accelerometers underwent multiple movements and subsequent recoveries due to alternating high-energy and calm hydrodynamic conditions during the monitoring period (Fig. 5c). The MI of the mussel clusters at all five locations increased nonlinearly with increasing near-bed orbital velocity (Fig. 6). As expected, subtidal mussel beds with different geographical distributions exhibited varying mobility thresholds, with values of 0.40 m s^{-1} for L1, 0.34 m s^{-1} for L2, 0.24 m s^{-1} for L4, 0.20 m s^{-1} for L5, and 0.29 m s^{-1} for L6, respectively (Fig. 6).

To identify the key factors driving the variations in mobility thresholds among locations, the average orbital velocity was excluded because of its significant correlation with elevation (Fig. 7a) and the relatively weaker explanatory potential for mobility threshold variability was compared to elevation (Fig. 7b). The resulting relationship between elevation and mobility threshold enabled the interpolation of mobility threshold for subtidal mussel beds (with elevations between −3.4 to −1.2 m Normal Amsterdam Level) in the Dutch Wadden Sea based on the digital elevation map (Fig. 8a,b).

Stability of subtidal mussel beds in the Dutch Wadden Sea

The return interval statistics for site-specific mobility thresholds revealed a notable spatial variability in the stability of the subtidal mussel beds (Fig. 8c). Shorter return intervals of mobility thresholds, such as a few days, indicate frequent mussel movement, categorizing areas as having a high risk of instability. Conversely, longer return intervals of mobility thresholds, up to 100 d, classify the locations as having a low risk of instability, rare mussel movements, and sufficient

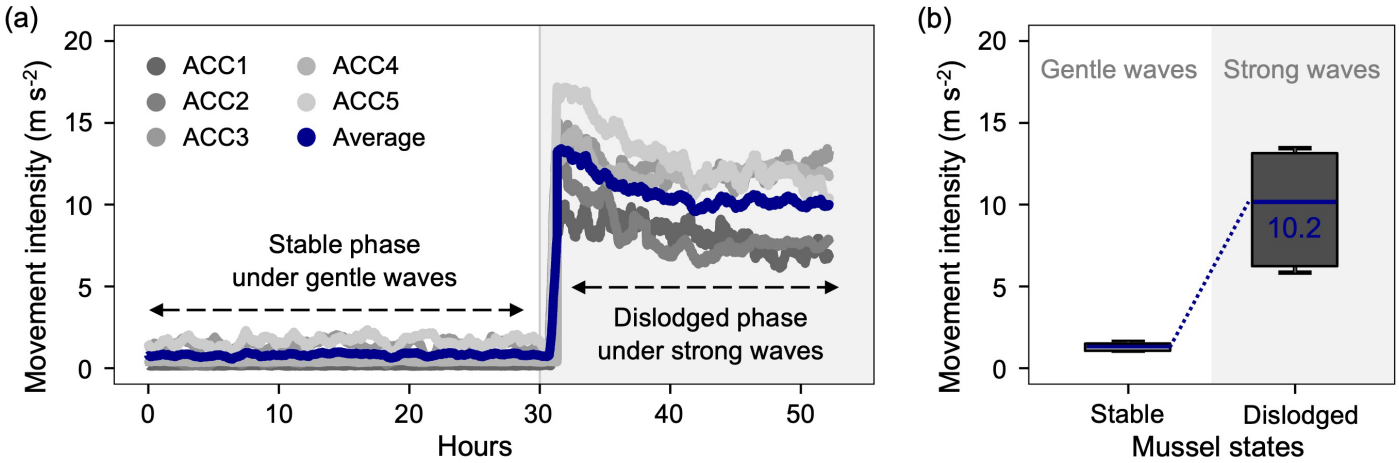

Fig. 4. (**a**) Calibration results on accelerometers (ACC) from flume tests show the stable state of mussel clusters during the acclimation phase (i.e., under gentle waves with a near-bed orbital velocity of 0.24 ± 0.01 m s^{-1}) and their movement state after exposure to increased near-bed orbital velocity (0.47 ± 0.02 m s^{-1}) under strong waves. Numbers in the legend represent individual ACC. "Average" denotes the average results of the five ACCs. (**b**) Statistical results for the movement intensity of mussel clusters in both stable and dislodged phases. The average movement intensity during the dislodged phase (i.e., 10.2 m s^{-2}, as indicated by the blue solid line in the box plot) is considered the representative movement intensity for mussel clusters in motion. If the movement intensity exceeds 10.2 m s^{-2}, the mussel clusters are considered to be in the movement state.

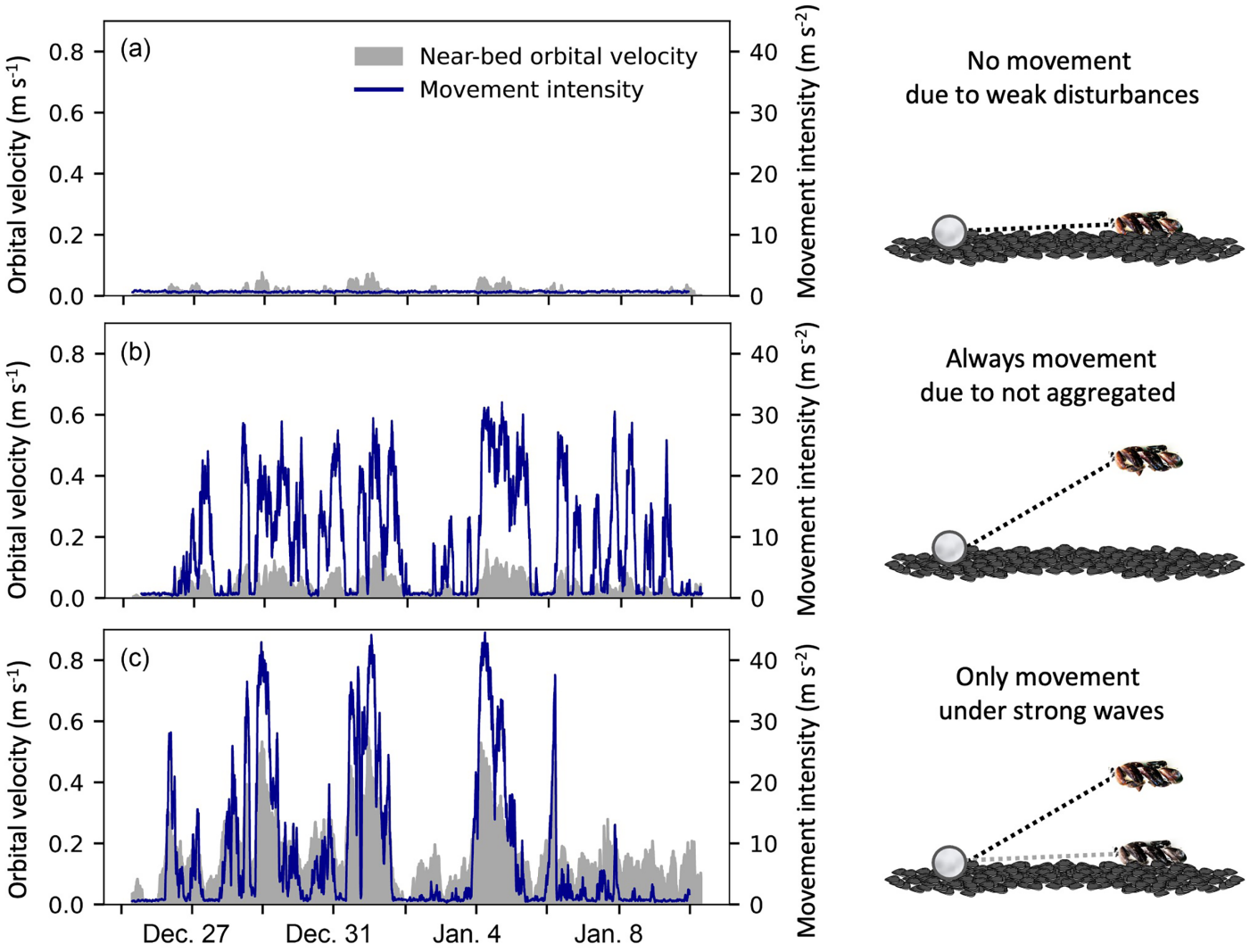

Fig. 5. Examples of data from Biophys loggers. (**a**) Mussel clusters containing accelerometers aggregated into the local mussel bed without movement due to weak orbital velocity (case from L8; Fig. 2b); (**b**) Mussel clusters containing accelerometers failed to aggregate into the local mussel beds because they remained in motion regardless of orbital velocity (case from L7; Fig. 2b); (**c**) Mussel clusters containing accelerometers aggregated into local mussel beds and were only moved under stronger orbital velocities (case from L5; Fig. 2b). Data are presented as location averages, with time truncated to enhance detail visibility.

recovery time. In general, a larger mobility threshold corresponded to a longer return interval, which was typically detected at sites with higher elevations (Fig. 8d). This finding suggests that mussel beds located at higher elevations tended to be more stable in the subtidal zone. Conversely, mussel beds at lower elevations were relatively unstable because mussel clusters were more prone to dislodgement because of lower mobility thresholds and shorter return intervals (Fig. 8d).

A significant correlation was found between the stability assessment and the on-site population loss rates (Fig. 9). Areas identified as having a lower instability risk were consistently aligned with locations with lower population loss rates and vice versa. This supports the credibility of the resulting stability assessment map.

Discussion

Adaptive responses shape the stability of subtidal soft-bottom mussel beds

The observed variations in mobility thresholds among subtidal soft-bottom mussel beds in this study showed a positive correlation with bed elevation, potentially stemming from adaptive responses (i.e., adjustments in behavior, physiology, or structure that help an organism cope with environmental stressors or changes; Miner et al. 2005) of mussels among those beds. Essentially, water is generally shallower at higher bed elevations within a region, which results in the slowing of wave speeds, enlargement of waveforms, and intensification of bottom friction, typically signaling stronger near-bed

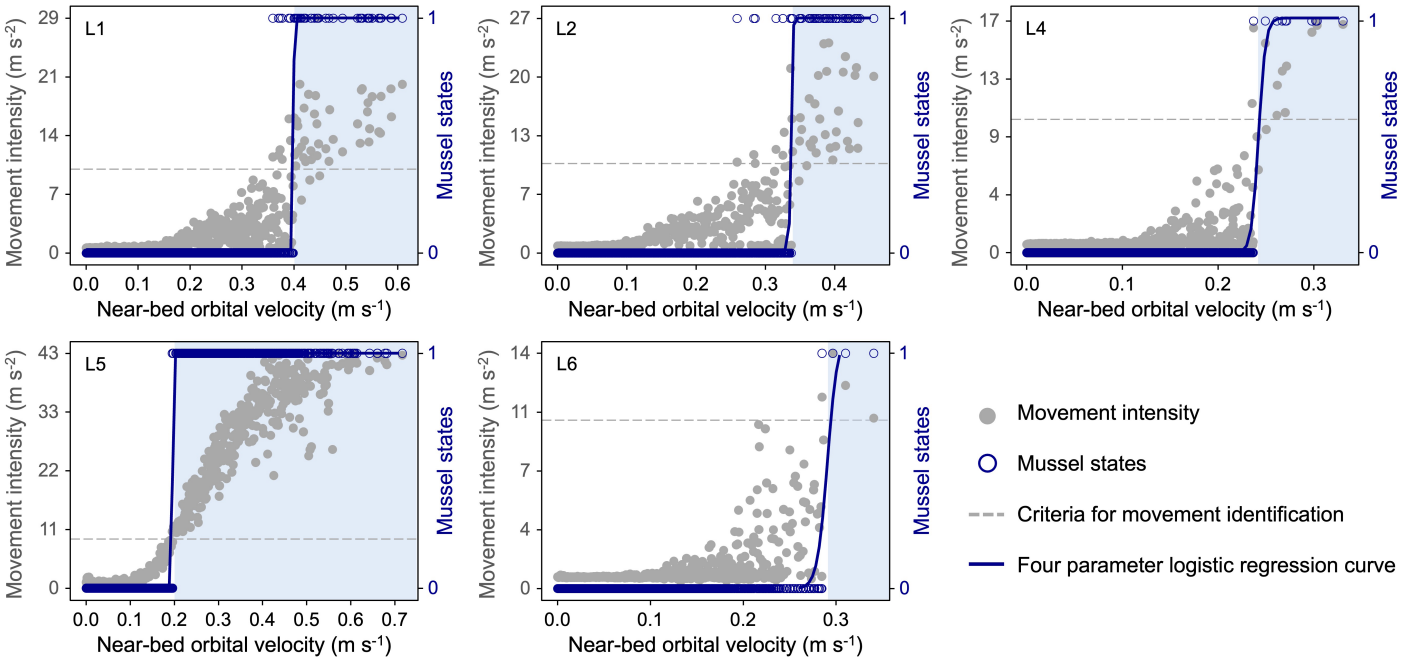

Fig. 6. The movement intensity of mussel clusters at varying near-bed orbital velocities, which were further categorized into the states of mussel clusters based on movement identification criteria—0 indicates a stable state, while 1 denotes a dislodged state. Labels in the top-left corners of subplots specify the locations of data acquisition (see Fig. 2b for geographic distribution). The mobility threshold, defined as the near-bed orbital velocity at which mussel cluster states undergo an abrupt shift, was determined using logistic regressions (R^2: 0.85, 0.83, 0.92, 0.99, and 0.81 for L1, L2, L4, L5, and L6, respectively) and represented by the inflection points of the logistic regression curves (0.40, 0.34, 0.24, 0.20, and 0.29 m s^{-1} for L1, L2, L4, L5, and L6, respectively). The light-blue background highlights the motion of mussel clusters beyond the mobility threshold.

hydrodynamic disturbances (Shi et al. 2019; Wei and Davison 2022). Strengthening of hydrodynamic stresses can potentially induce a response in individual mussels, manifesting as increased stress tolerance (i.e., the ability of an organism to endure or withstand stressors or adverse conditions without significant adverse effects; Miner et al. 2005). This increased tolerance can be achieved by allocating more energy to the production of stronger byssal threads or by increasing aggregation as they grow toward each other and coalesce (Connor and Robles 2015; Manríquez et al. 2021). The latter could trigger complex spatial patterns that further strengthen the stress tolerance of mussel beds,

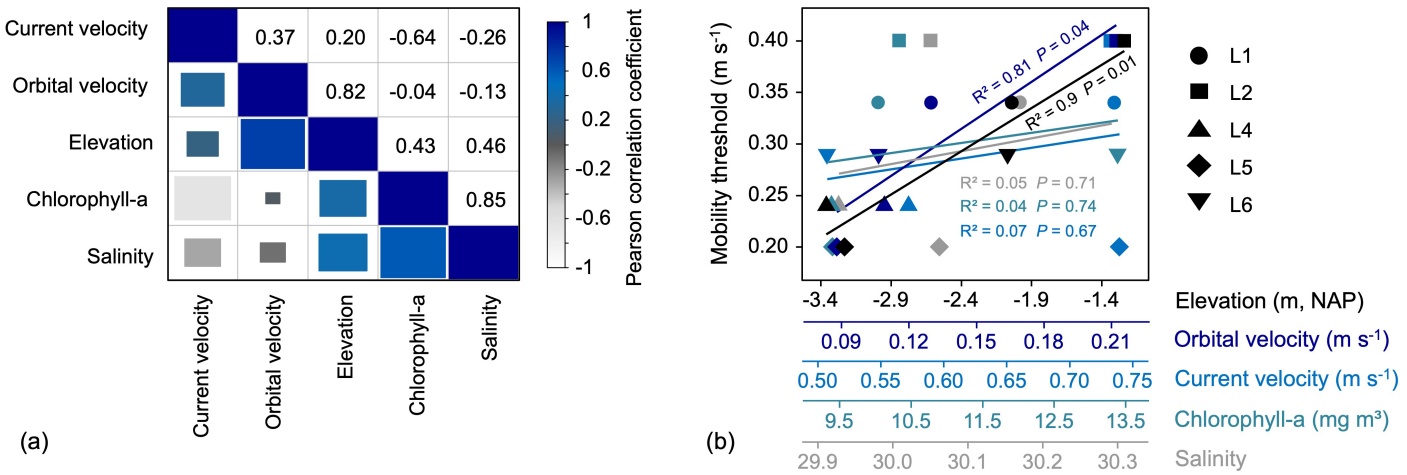

Fig. 7. (**a**) Results of the Pearson correlation for the five environmental variables. (**b**) Linear relationships between the five environmental variables and the mobility threshold of mussel beds (derived from Fig. 6). Different colors represent distinct environmental variables, while various shapes denote different locations (see geographic distribution in Fig. 2b). Each environmental variable is displayed with its independent *x*-axis corresponding to its respective color.

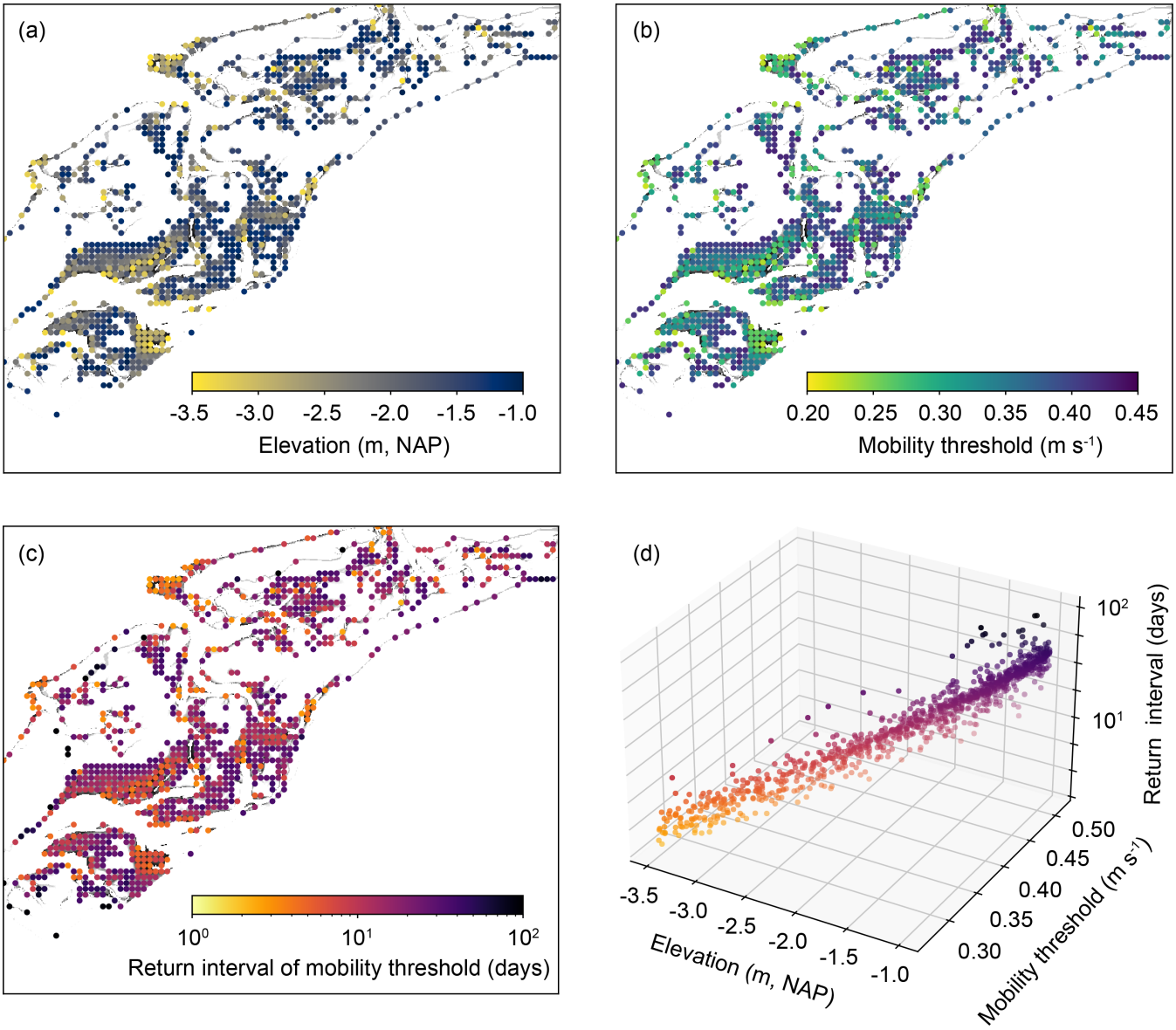

Fig. 8. (**a**) Digital elevation map of the subtidal zone (between −3.4 and −1.2 m Normal Amsterdam Level) in the Dutch Wadden Sea. (**b**) Mobility thresholds for subtidal mussel beds, which were interpolated using the linear relationship between elevation and mobility threshold derived in Fig. 7b. (**c**) Return interval of site-specific mobility threshold calculated by the wave model, serving as a quantitative indicator of mussel bed stability. Longer return intervals indicate lower instability risk, while shorter return intervals indicate higher instability risk. (**d**) Return interval of site-specific mobility threshold as a function of local elevation and mobility threshold.

depending on site-specific density and overall coverage (Commito et al. 2014). Increased stress tolerance to hydrodynamic disturbances imparts stability to the mussel bed, which, as an emergent structure, has the potential to attenuate local hydrodynamics (Koppel et al. 2005; Liu et al. 2014), thereby facilitating faster growth among individual mussels. When the bed elevation was lower (i.e., deeper water), the scenario flipped. Mussels may invest less in stress tolerance as they thrive in calm, low-stress environments.

The linear relationship between mussel motility and bed elevation, established in this study, holds true only within the elevation range covered by the field monitoring. Distinct patterns may emerge in regions with higher or lower bed elevations. For instance, in intertidal mussel beds, higher elevations imply longer exposure to air, which may diminish mussel stress tolerance by reducing byssal thread strength (Connor and Robles 2015; Schotanus et al. 2019), leading to decreased stability under high-energy hydrodynamic disturbances.

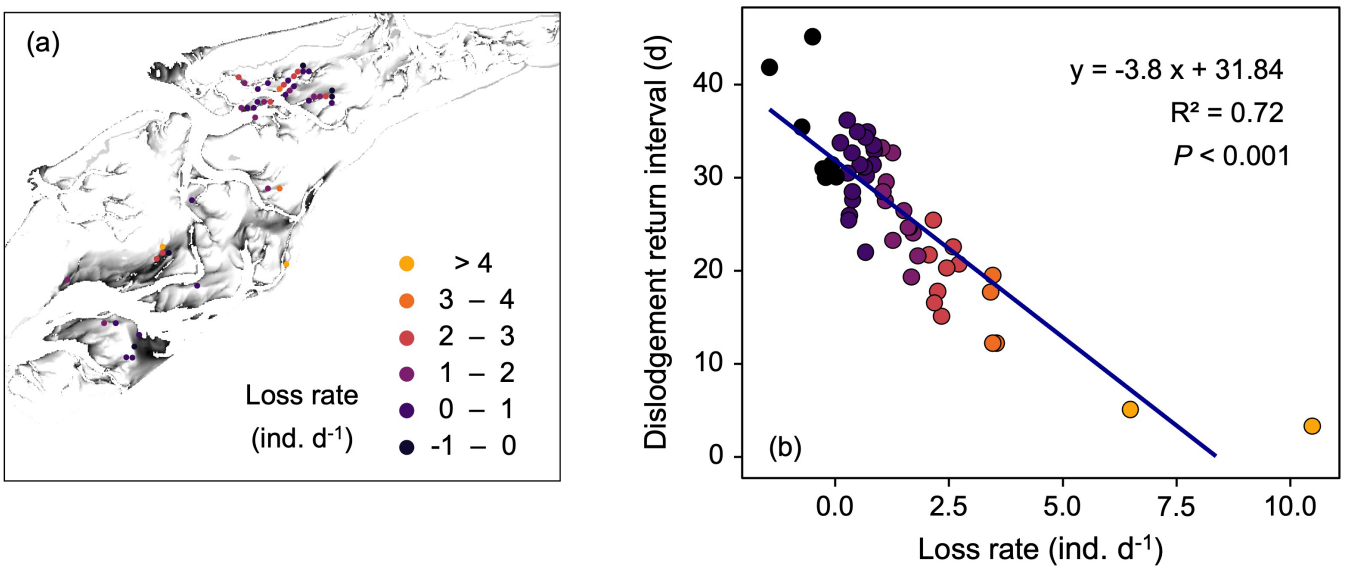

Fig. 9. (**a**) Geographic distribution of sites where mussel population loss rates were recorded in situ (data from Capelle et al. 2016). (**b**) Correlation between population loss rates and mobility threshold return intervals, which were extracted based on geographical locations in Fig. 8c.

Therefore, conducting similar research across a broader spectrum of bed elevations would be informative. Nevertheless, the stability of mussel beds depends on the balance between mussel stress tolerance to hydrodynamic forces and instantaneous hydrodynamic intensity (Carrington et al. 2009). Other factors that might influence mussel byssal thread strength, such as predator pressure (Manríquez et al. 2021), mussel age/relay time (Schotanus et al. 2019), substrate type (Christensen et al. 2015), and seasonality (Moeser et al. 2006), can further modulate mussel stress tolerance to hydrodynamic disturbances, consequently influencing mussel stability. The size and density of individual mussel beds, as well as the spacing between them, may also indirectly influence mussel adaptive responses and bed stability by modifying local abiotic conditions (de Paoli et al. 2015; Capelle et al. 2016). This effect is known as scale-dependent feedback (Koppel et al. 2005), as observed by the attenuation of hydrodynamic disturbances at the center of the mussel bed and their amplification at its edges or between the beds (Donker 2015). Overall, the potential of mussel responses to stabilize mussel beds may be context-dependent, which echoes previous studies discussing the role of pre-existing conditions in shaping ecosystem resilience (Frieder et al. 2014; Thayne et al. 2022).

Mobility under regular disturbances informs stability under extreme disturbances

The quantification of critical thresholds that trigger ecosystem changes is challenging (Hillebrand et al. 2020; Rietkerk et al. 2021). For instance, the hydrodynamic-induced collapse of subtidal soft-bottom mussel beds requires extreme storm events (de Paoli et al. 2015; Manríquez et al. 2021), which may be difficult to monitor. Our study shifted the focus to examining the hydrodynamic threshold driving the rapid increase in mussel mobility (Fig. 1). In this context, mussels in motion may either engage in short-distance rolling and re-aggregation during subsequent calm hydrodynamic periods (Bertolini et al. 2019) or undergo long-distance displacement in response to stronger hydrodynamic forces. The more frequently the mobility threshold is surpassed under typical hydrodynamic conditions, the more fragmented and less stable the mussel bed becomes (Donker 2015), thereby increasing the risk of collapse during extreme hydrodynamic events. The robust correlation between our assessment results on mussel bed stability and the documented population loss rates of mussel beds in the literature provides persuasive evidence.

Our assessment of mussel bed stability in the Dutch Wadden Sea may be somewhat conservative as it relies on insights derived from commercial mussel beds to estimate mobility thresholds. These estimated thresholds may not fully reflect the actual conditions in wild mussel beds, where the variation in the age and size of mussels and the rougher bottom topography would affect the strength of mussel byssal threads (Nehls and Thiel 1993; Christensen et al. 2015; Manríquez et al. 2021). Despite this limitation, our device has the potential for broader applications in future studies. The resulting stability map can help identify vulnerable areas where mussel beds are at greater risk of fragmentation or collapse during extreme hydrodynamic events. Such insights would facilitate targeted management efforts to minimize risks, such as strengthening mussel stress tolerance to hydrodynamic disturbances through substrate modifications (Schotanus et al. 2020; Temmink et al. 2021) or introducing native mussels from aquaculture to aid the recovery process (Wilcox et al. 2018). Moreover, our study revealed the role of

bed elevation in shaping the stress tolerance of mussels to hydrodynamic disturbances. These findings are relevant to the management of mussel beds. Mussels in soft-bottom systems have been documented to form byssal threads within minutes and aggregate with conspecifics within hours (Commito et al. 2014), suggesting that outplanted mussels may retain their original mobility thresholds during the early stages of establishment, thus maintaining stability. In the long term, the strength of new byssal threads may decrease as the mussels would subsequently respond to calmer hydrodynamic conditions at the outplacement sites; however, this weakening could be partially offset by mussel growth (e.g., the production of more byssal threads and an increase in shell area for attachment). Further research is needed to gain insight into the temporal variability of the mussel mobility threshold, given its importance in interpreting management outcomes and refining strategies. Nevertheless, as we obtained mussel mobility thresholds in the field during an average wind year, we expected the observed trends with elevation to be representative of typical current conditions.

Author Contributions

Zhiyuan Zhao, Jaco C. de Smit, Jacob J. Capelle, and Tjeerd J. Bouma contributed to conception and design. Zhiyuan Zhao, Jaco C. de Smit, Jacob J. Capelle, and Mingxuan Wu contributed to the acquisition of data. Zhiyuan Zhao, Jaco C. de Smit, Jacob J. Capelle, and Tim Grandjean contributed to the analysis and interpretation of data. Zhiyuan Zhao, Jaco C. de Smit, Jacob J. Capelle, Tim Grandjean, Mingxuan Wu, Theo Gerkema, Johan van de Koppel, and Tjeerd J. Bouma drafted and/or revised the article. Zhiyuan Zhao, Jaco C. de Smit, Jacob J. Capelle, Tim Grandjean, Mingxuan Wu, Theo Gerkema, Johan van de Koppel, and Tjeerd J. Bouma approved the submitted version for publication.

Acknowledgments

The authors thank Wouter Suykerbuyk for assistance in fieldwork. This work is part of the Dynamos project, which is funded by the European Fisheries Fund, in collaboration with the Producers' Organization of Dutch Mussel culture (POM).

Conflicts of Interest

None declared.

References

Avdelas, L., E. Avdic-Mravlje, A. C. Borges Marques, et al. 2021. "The Decline of Mussel Aquaculture in the European Union: Causes, Economic Impacts and Opportunities." *Reviews in Aquaculture* 13: 91–118. https://doi.org/10.1111/raq.12465.

Bertolini, C., B. Cornelissen, J. Capelle, J. Van De Koppel, and T. J. Bouma. 2019. "Putting Self-Organization to the Test: Labyrinthine Patterns as Optimal Solution for Persistence." *Oikos* 128: 1805–1815. https://doi.org/10.1111/oik.06373.

Bridger, D., M. J. Attrill, B. F. Davies, et al. 2022. "The Restoration Potential of Offshore Mussel Farming on Degraded Seabed Habitat." *Aquaculture, Fish and Fisheries* 2: 437–449. https://doi.org/10.1002/aff2.77.

Capelle, J. J., L. Leuchter, M. de Wit, E. Hartog, and T. J. Bouma. 2019. "Creating a Window of Opportunity for Establishing Ecosystem Engineers by Adding Substratum: A Case Study on Mussels." *Ecosphere* 10: e02688. https://doi.org/10.1002/ecs2.2688.

Capelle, J. J., M. R. Van Stralen, J. W. Wijsman, P. M. Herman, and A. C. Smaal. 2017. "Population Dynamics of Subtidal Blue Mussels *Mytilus edulis* and the Impact of Cultivation." *Aquaculture Environment Interactions* 9: 155–168. https://doi.org/10.3354/aei00221.

Capelle, J. J., J. W. Wijsman, M. R. Van Stralen, P. M. Herman, and A. C. Smaal. 2016. "Effect of Seeding Density on Biomass Production in Mussel Bottom Culture." *Journal of Sea Research* 110: 8–15. https://doi.org/10.1016/j.seares.2016.02.001.

Carrington, E., G. M. Moeser, J. Dimond, J. J. Mello, and M. L. Boller. 2009. "Seasonal Disturbance to Mussel Beds: Field Test of a Mechanistic Model Predicting Wave Dislodgment." *Limnology and Oceanography* 54: 978–986. https://doi.org/10.4319/lo.2009.54.3.0978.

Christensen, H. T., P. Dolmer, B. W. Hansen, et al. 2015. "Aggregation and Attachment Responses of Blue Mussels, *Mytilus Edulis*—Impact of Substrate Composition, Time Scale and Source of Mussel Seed." *Aquaculture* 435: 245–251. https://doi.org/10.1016/j.aquaculture.2014.09.043.

Commito, J. A., B. R. Jones, M. A. Jones, S. E. Winders, and S. Como. 2018. "What Happens after Mussels Die? Biogenic Legacy Effects on Community Structure and Ecosystem Processes." *Journal of Experimental Marine Biology and Ecology* 506: 30–41. https://doi.org/10.1016/j.jembe.2018.05.004.

Commito, J. A., A. E. Commito, R. V. Platt, et al. 2014. "Recruitment Facilitation and Spatial Pattern Formation in Soft-Bottom Mussel Beds." *Ecosphere* 5: 1–26. https://doi.org/10.1890/ES14-00200.1.

Connor, K. M., and C. D. Robles. 2015. "Within-Site Variation of Growth Rates and Terminal Sizes in *Mytilus californianus* Along Wave Exposure and Tidal Gradients." *The Biological Bulletin* 228: 39–51. https://doi.org/10.1086/BBLv228n1p39.

Crotty, S. M., D. Pinton, A. Canestrelli, et al. 2023. "Faunal Engineering Stimulates Landscape-Scale Accretion in Southeastern US Salt Marshes." *Nature Communications* 14: 881. https://doi.org/10.1038/s41467-023-36444-w.

de Paoli, H., J. van de Koppel, E. van der Zee, et al. 2015. "Processes Limiting Mussel Bed Restoration in the Wadden-Sea." *Journal of Sea Research* 103: 42–49. https://doi.org/10.1016/j.seares.2015.05.008.

De Paoli, H., T. Van Der Heide, A. Van Den Berg, et al. 2017. "Behavioral Self-Organization Underlies the Resilience of a

Coastal Ecosystem." *Proceedings of the National Academy of Sciences of the United States of America* 114: 8035–8040. https://doi.org/10.1073/pnas.1619203114.

Donker, J. J. A. 2015. "Hydrodynamic Processes and the Stability of Intertidal Mussel Beds in the Dutch Wadden Sea." Doctoral diss., Utrecht University, Faculty of Geosciences.

Donker, J. J. A., M. Van der Vegt, and P. Hoekstra. 2013. "Wave Forcing Over an Intertidal Mussel Bed." *Journal of Sea Research* 82: 54–66. https://doi.org/10.1016/j.seares.2012.08.010.

Frieder, C. A., J. P. Gonzalez, E. E. Bockmon, et al. 2014. "Can Variable pH and Low Oxygen Moderate Ocean Acidification Outcomes for Mussel Larvae?" *Global Change Biology* 20: 754–764. https://doi.org/10.1111/gcb.12485.

Hawkins, S. J., M. T. Burrows, and N. Mieszkowska. 2023. "Shoreline Sentinels of Global Change Show the Consequences of Extreme Events." *Global Change Biology* 29: 7. https://doi.org/10.1111/gcb.16477.

Hillebrand, H., I. Donohue, W. S. Harpole, et al. 2020. "Thresholds for Ecological Responses to Global Change Do Not Emerge From Empirical Data." *Nature Ecology & Evolution* 4: 1502–1509. https://doi.org/10.1038/s41559-020-1256-9.

van de Koppel, J., M. Rietkerk, N. Dankers, and P. M. Herman. 2005. "Scale-Dependent Feedback and Regular Spatial Patterns in Young Mussel Beds." *American Naturalist* 165: E66–E77. https://doi.org/10.1086/428362.

Kossin, J. P., K. R. Knapp, T. L. Olander, and C. S. Velden. 2020. "Global Increase in Major Tropical Cyclone Exceedance Probability Over the Past Four Decades." *Proceedings of the National Academy of Sciences of the United States of America* 117: 11975–11980. https://doi.org/10.1073/pnas.1920849117.

Liu, Q. X., P. M. Herman, W. M. Mooij, et al. 2014. "Pattern Formation at Multiple Spatial Scales Drives the Resilience of Mussel Bed Ecosystems." *Nature Communications* 5: 5234. https://doi.org/10.1038/ncomms6234.

Manríquez, P. H., M. E. Jara, C. P. González, et al. 2021. "The Combined Effects of Climate Change Stressors and Predatory Cues on a Mussel Species." *Science of the Total Environment* 776: 145916. https://doi.org/10.1016/j.scitotenv.2021.145916.

Miner, B. G., S. E. Sultan, S. G. Morgan, D. K. Padilla, and R. A. Relyea. 2005. "Ecological Consequences of Phenotypic Plasticity." *Trends in Ecology & Evolution* 20: 685–692. https://doi.org/10.1016/j.tree.2005.08.002.

Moeser, G. M., H. Leba, and E. Carrington. 2006. "Seasonal Influence of Wave Action on Thread Production in *Mytilus edulis*." *Journal of Experimental Biology* 209: 881–890. https://doi.org/10.1242/jeb.02050.

Nehls, G., and M. Thiel. 1993. "Large-Scale Distribution Patterns of the Mussel *Mytilus Edulis* in the Wadden Sea of Schleswig-Holstein: Do Storms Structure the Ecosystem?" *Netherlands Journal of Sea Research* 31: 181–187. https://doi.org/10.1016/0077-7579(93)90008-G.

Neilson, E. W., C. T. Lamb, S. M Konkolics, et al. 2020. "There's a Storm a-Coming: Ecological Resilience and Resistance to Extreme Weather Events." *Ecology and Evolution* 10: 12147–12156. https://doi.org/10.1002/ece3.6842.

Ricklefs, K., H. Büttger, and H. Asmus. 2020. "Occurrence, Stability, and Associated Species of Subtidal Mussel Beds in the North Frisian Wadden Sea." *Estuarine, Coastal and Shelf Science* 233: 106549. https://doi.org/10.1016/j.ecss.2019.106549.

Rietkerk, M., R. Bastiaansen, S. Banerjee, et al. 2021. "Evasion of Tipping in Complex Systems Through Spatial Pattern Formation." *Science* 374: eabj0359. https://doi.org/10.1126/science.abj0359.

Scheffer, M., S. R. Carpenter, T. M. Lenton, et al. 2012. "Anticipating Critical Transitions." *Science* 338: 344–348. https://doi.org/10.1126/science.1225244.

Schotanus, J., J. J. Capelle, L. Leuchter, J. Van De Koppel, and T. J. Bouma. 2019. "Mussel Seed Is Highly Plastic to Settling Conditions: The Influence of Waves Versus Tidal Emergence." *Marine Ecology Progress Series* 624: 77–87. https://doi.org/10.3354/meps13039.

Schotanus, J., J. J. Capelle, E. Paree, et al. 2020. "Restoring Mussel Beds in Highly Dynamic Environments by Lowering Environmental Stressors." *Restoration Ecology* 28: 1124–1134. https://doi.org/10.1111/rec.13168.

Shi, B., J. R. Cooper, J. Li, et al. 2019. "Hydrodynamics, Erosion and Accretion of Intertidal Mudflats in Extremely Shallow Waters." *Journal of Hydrology* 573: 31–39. https://doi.org/10.1016/j.jhydrol.2019.03.065.

Smaal, A. C., J. A. Craeymeersch, and M. R. Van Stralen. 2021. "The Impact of Mussel Seed Fishery on the Dynamics of Wild Subtidal Mussel Beds in the Western Wadden Sea, the Netherlands." *Journal of Sea Research* 167: 101978. https://doi.org/10.1016/j.seares.2020.101978.

Soulsby, R. 2006. Simplified Calculation of Wave Orbital Velocities. Tech. Rep. Wallingford, UK: HR Wallingford Ltd.

Temmink, R. J., C. Angelini, G. S. Fivash, et al. 2021. "Life Cycle Informed Restoration: Engineering Settlement Substrate Material Characteristics and Structural Complexity for Reef Formation." *Journal of Applied Ecology* 58: 2158–2170. https://doi.org/10.1111/1365-2664.13968.

Temmink, R. J., L. P. Lamers, C. Angelini, et al. 2022. "Recovering Wetland Biogeomorphic Feedbacks to Restore the World's Biotic Carbon Hotspots." *Science* 376: eab1479. https://doi.org/10.1126/science.abn1479.

Thayne, M. W., B. M. Kraemer, J. P. Mesman, B. W. Ibelings, and R. Adrian. 2022. "Antecedent Lake Conditions Shape Resistance and Resilience of a Shallow Lake Ecosystem Following Extreme Wind Storms." *Limnology and Oceanography* 67: S101–S120. https://doi.org/10.1002/lno.11859.

Troost, K., J. van der Meer, and M. van Stralen. 2022. "The Longevity of Subtidal Mussel Beds in the Dutch Wadden Sea." *Journal of Sea Research* 181: 102174. https://doi.org/10.1016/j.seares.2022.102174.

Wang, S., and R. Toumi. 2022. "More Tropical Cyclones Are Striking Coasts with Major Intensities at Landfall." *Scientific*

Reports 12: 5236. https://doi.org/10.1038/s41598-022-09287-6.

Wei, Z., and A. Davison. 2022. "A Convolutional Neural Network Based Model to Predict Nearshore Waves and Hydrodynamics." *Coastal Engineering* 171: 104044. https://doi.org/10.1016/j.coastaleng.2021.104044.

Wilcox, M., S. Kelly, and A. Jeffs. 2018. "Ecological Restoration of Mussel Beds Onto Soft-Sediment Using Transplanted Adults." *Restoration Ecology* 26: 581–590. https://doi.org/10.1111/rec.12607.

Young, I. R., and L. A. Verhagen. 1996. "The Growth of Fetch Limited Waves in Water of Finite Depth. Part 1. Total Energy and Peak Frequency." *Coastal Engineering* 29: 47–78. https://doi.org/10.1016/S0378-3839(96)00006-3.

Zhao, Z., J. J. Capelle, J. C. de Smit, et al. 2024. "Boosting Efficiency of Mussel Spat Collection for Ecological Sustainability: Identifying Critical Drivers and Informing Management." *Journal of Applied Ecology* 61: 1691–1702. https://doi.org/10.1111/1365-2664.14696.

Zhao, Z., L. Zhang, L. Yuan, and T. J. Bouma. 2022. "Unraveling the Wheel of Recruitment for Salt-Marsh Seedlings: Resistance to and Recovery After Dislodgement." *Science of the Total Environment* 847: 157595. https://doi.org/10.1016/j.scitotenv.2022.157595.

Supporting Information

Additional Supporting Information may be found in the online version of this article.

Submitted 06 April 2024
Revised 23 September 2024
Accepted 02 February 2025